Natural convection of Casson fluid in a square enclosure

M S Aghighi, Christel Metivier, H Masoumi

Natural convection of Casson fluid in a square enclosure

M. S. Aghighi [a,*], C. Metivier [b] , A. Ammar [c], H. Masoumi[a]

[a] *Department of Mechanical Engineering, Bu-Ali Sina University, 65175-38695 Hamedan, Iran*

[b] *LEMTA, UMR 7563, 2 Avenue de la Forêt de Haye, TSA 60604, 54518 Vandoeuvre les Nancy, France*

[c] *Arts et Métiers ParisTech, 2 Boulevard du Ronceray, BP 93525, F-49035 Angers cedex 01, France*

** Corresponding author: Tel.: +98-811-8273952; Fax: +98-811-8273952*

E-mail address: ms.aghighi@gmail.com ; christel.metivier@univ-lorraine.fr; Amine.Ammar@ensam.eu

Natural convection of Casson fluid in a square enclosure

Abstract

In this paper, natural convection of a yield stress fluid is studied in a square enclosure with differentially heated side walls. In particular, we consider the Casson model which is a commonly used model. The system is solved numerically by Galerkin's weighted residuals scheme of finite element method. Results of both Casson and Bingham models are presented and compared. Nominal values of Rayleigh number are in the range $10^3 - 10^6$and the Prandtl number is fixed to Pr =100 since results are not sensitive to Pr in the tested range $10 - 10^3$. Results highlight a larger degree of the shear-thinning in the Bingham case than in the Casson one. We show that the yield stress has a stabilizing effect since the convection can stop for yield stress fluids while this is not the case for Newtonian fluids. In the case of yield stress fluids, the flow becomes motionless above a critical yield number Y_c because the plug regions invade the whole cavity. The value of Y_c obtained with the Bingham model is larger than the one obtained with the Casson model. For both fluids, results highlight a weak dependence of Y_c with the Rayleigh number: $Y_c \sim Ra^{0.03}$ for Bingham fluids and $Y_c \sim Ra^{0.07}$ for Casson fluids. A supercritical bifurcation at the transition between the convective and the conductive regimes is found for both Bingham and Casson models. New correlations are proposed for the mean Nusselt number $\overline{Nu}$ for both Casson and Bingham fluids.

Keywords: Natural convection, Yield stress, Casson model, Bingham model, Finite element.

1. Introduction

Natural convection in enclosures is one of the most extensively studied configuration. Several systems and industrial processes (such as energy transfer in rooms and buildings, heat exchangers, electronic cooling, solar collectors, etc.) are based on natural convection, justifying the impressive volume of work devoted to its understanding during more than one century. Over this period, numerous studies related to Newtonian fluids have been done, extensive reviews have been made by Ostrach [1] and Bejan [2] where different boundary conditions are studied. Our concern focuses on the natural convection induced by a horizontal temperature gradient, i.e. a fluid layer heated from side wall. When considering viscous fluids, the flow consists in a convective regime provided that the temperature difference between the two vertical walls is not equal to zero.

For non-Newtonian fluids, Lamsaadi and Naimi [3] are the first to consider power law fluids in a vertical rectangular cavity heated from side walls. More recently, Turan et al. [4] analyzed two-dimensional laminar natural convection of power law fluids in square enclosures with differentially heated side walls. In the case of yield stress fluids, natural convection in rectangular enclosures have been numerically studied in Lyubimova [5], Vikhansky [6] when considering a Bingham fluid. These studies highlight the cessation of convection above a critical yield number while this is not the case for Newtonian fluids case. The unsteady cessation of convection in a Bingham fluid is also demonstrated in Karimfazli et al [7]. The heat transfer has been studied in a regularized biviscosity model by Turan et al [8], [9]for rectangular and square enclosures using FLUENT. Without any regularization of the Bingham constitutive law, Vola et al. [10] and Huilgol and Kefayati [11] have implemented this benchmark configuration by using respectively an augmented Lagrangian method and the operator splitting method. All these latter articles have studied the natural convection in Bingham fluids when submitted to a horizontal temperature gradient. The Bingham model is the most common used model because it is the simplest yield stress fluid model. However another simple and common yield stress fluid is the Casson fluid [12].

Casson model was proposed by Casson [13] to describe the flow of mixtures of pigments and oil. This model is often used to describe the behavior of numerous materials such as biological ones (e.g. blood) and agro-food ones e.g. yoghurt, tomato puree, molten chocolate, etc. The flow behavior of some particulate suspensions can also be approximated by this model [14]. The Bingham and Casson models provide close but different rheological results such as values of viscosity at fixed shear rate. In the field of fluid flows, in particular natural convection, the Casson model is understudied while this model is often used to fit rheological behavior of yield stress fluids.

In this paper, we propose to study numerically the natural convection of viscoplastic fluids obeying the Casson model in square enclosures with differentially heated side walls. To our knowledge, this situation has never been studied before. For this purpose, a Galerkin's weighted residuals scheme of finite element method has been developed. Due to the difficulty to treat the transition between the solid-like to liquid-like behaviors, a regularized model is used. In addition, we propose to compare results obtained from both the Casson and Bingham models when a similar regularization is used.

An outline of this paper is as follows. In section 2, the problem is mathematically formulated. The numerical method is briefly outlined and validated in section 3. Results in terms of velocity and temperature fields are proposed in section 4.1. The flow structure is provided in § 4.2, in particular, the unyielded regions are defined. Heat transfer is studied in § 4.3. In the whole article a comparison between both Casson and Bingham models is provided, differences between the models are discussed. Finally, concluding remarks are given in the section 5.

2. Mathematical formulation

The geometry under analysis is depicted in Fig. 1. The two vertical walls are kept at different temperatures with T_H the temperature enforced at the left wall and T_C, the temperature of the right wall ($T_H > T_C$). The horizontal boundaries are considered to be adiabatic. Both velocity components (i.e. u for the horizontal component and v for the vertical one) are identically zero on each boundary because we consider no-slip conditions and impenetrability of the fluid at rigid boundaries. Assuming the Boussinesq approximation and using the following characteristic scales: H for length, $u_0 = (g\beta H\Delta T)^{1/2}$ for the velocity, and $p_0 = \rho u_0^2$ for the pressure, the dimensionless mass, momentum and energy equations for two-dimensional natural convection in a square cavity are:

$$\frac{\partial u}{\partial x} + \frac{\partial v}{\partial y} = 0$$

$$u\frac{\partial u}{\partial x} + v\frac{\partial u}{\partial y} = -\frac{\partial p}{\partial x} + Pr^{\frac{1}{2}}Ra^{\frac{-1}{2}}\left(\frac{\partial \tau_{xx}}{\partial x} + \frac{\partial \tau_{yx}}{\partial y}\right)$$

$$u\frac{\partial v}{\partial x} + v\frac{\partial v}{\partial y} = -\frac{\partial p}{\partial y} + Pr^{\frac{1}{2}}Ra^{\frac{-1}{2}}\left(\frac{\partial \tau_{yy}}{\partial y} + \frac{\partial \tau_{xy}}{\partial x}\right) + \theta \qquad (1)$$

$$u\frac{\partial \theta}{\partial x} + v\frac{\partial \theta}{\partial y} = (Ra.Pr)^{-1/2}\left(\frac{\partial^2 \theta}{\partial x^2} + \frac{\partial^2 \theta}{\partial y^2}\right)$$

Where θ and p are respectively the dimensionless temperature and pressure.

The dimensionless temperature θ is defined by:

$$\theta = \frac{T - T_r}{T_H - T_C} \qquad (2)$$

with T_r a reference temperature defined by $T_r = (T_H + T_C)/2$.

The Prandtl number, Pr, and Rayleigh number, Ra are defined by:

$$Pr = \frac{\mu}{\rho\alpha}$$

$$Ra = \frac{\rho g\beta\Delta T H^3}{\alpha\mu} \qquad (3)$$

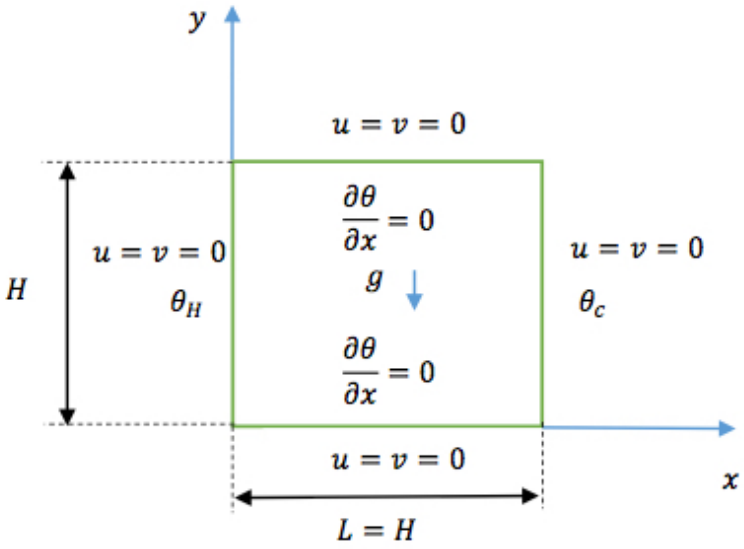

Fig. 1 Schematic diagram of the physical model and coordinate system.

where μ is the plastic viscosity, α is the thermal diffusivity, ρ is the density, g is the acceleration due to gravity, β is the coefficient of thermal expansion, and $\Delta T = T_H - T_C$ is the temperature difference between the hot and cold walls.

The boundary conditions for this problem are:

$$u = v = 0 \text{ at walls}$$

$$\frac{\partial \theta}{\partial x} = 0 \;\; at \;\; y = 0 \; and \; y = 1 \qquad (4)$$

$$\theta = 0.5 \quad at \; \mathrm{x} = 0$$

$$\theta = -0.5 \;\; at \;\; x = 1$$

The stress-deformation behavior of viscoplastic materials based on the Casson and Bingham models is given by:

For the Casson model:

$$\tau_{ij} = \left(1 + \left(\frac{Bn}{|\dot{\gamma}|}\right)^{\frac{1}{2}}\right)^2 \dot{\gamma}_{ij} \quad if \quad |\tau| > \tau_y \tag{5}$$

For the Bingham model:

$$\tau_{ij} = \left(1 + \left(\frac{Bn}{|\dot{\gamma}|}\right)\right)\dot{\gamma}_{ij} \quad if \quad |\tau| > \tau_y$$

and

$$\dot{\gamma} = 0 \quad for \quad |\tau| < \tau_y \tag{6}$$

for both models.

In Eqs. (5) and (6), $|\tau|$ and $|\dot{\gamma}|$ are the second invariant of the shear stress and the rate of strain tensors respectively, and Bn is the Bingham number defined by:

$$Bn = (Pr/Ra)^{-1/2} \frac{\tau_y}{\rho\beta g \Delta T H} = (Pr/Ra)^{-1/2} Y \tag{7}$$

with Y the yield number which corresponds to the ratio between the yield stress and the buoyancy effects $Y = \frac{\tau_y}{\rho\beta g \Delta T H}$. It is worth noting that the yield number Y does not depend on Ra and Pr contrary to Bn.

The component $\dot{\gamma}_{ij}$ of the rate-of-strain tensor is defined by:

$$\dot{\gamma}_{ij} = \frac{\partial u_i}{\partial x_j} + \frac{\partial u_j}{\partial x_i} \tag{8}$$

Finally, the second invariant of the rate of strain and stress tensors are given by

$|\dot{\gamma}| = \sqrt{\frac{1}{2}\dot{\gamma}_{ij}\dot{\gamma}_{ij}}$ and $|\tau| = \sqrt{\frac{1}{2}\tau_{ij}\tau_{ij}}$.

Papanastasiou modifications method [15] can be applied to Casson model to avoid the discontinuity between yielded and unyielded regions since the stress tensor is indeterminate when $|\tau| < \tau_y$ and the viscosity tends to infinity when $\dot{\gamma} \to 0$. To circumvent this difficulty, we use regularized models such as that one proposed by Papanastasiou. Based on this regularization,

Equations (5) and (6) are as follows:

$$\tau_{ij} = \left(1 + \left(\frac{Bn}{|\dot{\gamma}|}\right)^{\frac{1}{2}} (1 - \exp\left(-\sqrt{m|\dot{\gamma}|}\right)\right)^2 \dot{\gamma}_{ij} \quad (9)$$

for the Casson model and

$$\tau_{ij} = \left(1 + \left(\frac{Bn}{|\dot{\gamma}|}\right) (1 - \exp\left(-m|\dot{\gamma}|\right)\right) \dot{\gamma}_{ij} \quad (10)$$

for the Bingham model.

In Equations (9) and (10), m is a regularization parameter, it allows to converge to a finite value of the viscosity when $\dot{\gamma} \to 0$ and it provides a continuous law for the stress tensor whatever the values of $\dot{\gamma}$ and τ. In the Bingham case, at low shear rate ($\dot{\gamma} \to 0$) the viscosity tends to $\mu = 1 + m\,Bn$, in the Casson case it tends to $\mu = 1 + m\,Bn + \sqrt{mBn}$. The viscosity at low or zero shear rate depends on the Bingham number but also on the regularization parameter. Because the Bingham or Casson models without any regularization lead to infinite viscosity when $\dot{\gamma} \to 0$, the value of m is usually chosen to be large, in this study we set $m = 10^4$. For this value of m, the regularized Bingham and Casson models present values of viscosity close to that of the non-regularized respective models when $\dot{\gamma} > 10^{-4}$. The Figure 2 represents the viscosity as a function of the shear rate for the Bingham and the Casson models. At low and high shear rate values, the two models lead to close values of viscosity. The main difference sets in the shear thinning behavior. One notices that the Bingham model presents a more abrupt decrease in viscosity than in the case of the Casson model. In other words, it means that the shear-thinning degree α, which could be characterized by the derivative of the viscosity with respect to $\dot{\gamma}$, i.e. $\alpha = \left|\frac{d\mu}{d\dot{\gamma}}\right|$, is larger in the Bingham model case than in the Casson one.

The heat flux averaged over the hot wall is defined via the Nusselt number:

$$\overline{Nu} = -\int_0^1 \left.\frac{\partial\theta}{\partial y}\right|_{y=0} dx \qquad (11)$$

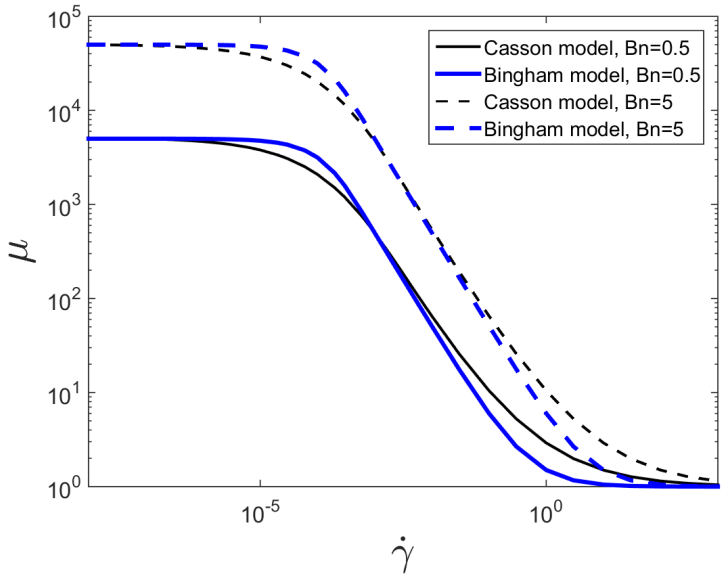

Fig. 2 Variations of the viscosity with the shear rate for the Bingham and the Casson models.

3. Numerical analysis

3.1. Method of solution

Numerical solutions of the coupled conservation equations of mass, momentum and energy related to the two-dimensional steady state natural convection within square enclosures are obtained by developing a numerical code based on the Galerkin weighted residual finite element method with quadrilateral, eight nodes elements. The Galerkin weak statement is obtained by minimizing the residual error over the discretized domain[16]. As in Aghighi et al. [17] in what follows we consider a penalty formulation of the incompressibility constraint. Thus, the equation (1) can be rewritten as below:

$$\frac{\partial u}{\partial x}+\frac{\partial v}{\partial y}+\frac{1}{\lambda}p=0$$

$$u\frac{\partial u}{\partial x}+v\frac{\partial u}{\partial y}+\frac{\partial p}{\partial x}=Pr^{\frac{1}{2}}Ra^{\frac{-1}{2}}\left(\frac{\partial \tau_{xx}}{\partial x}+\frac{\partial \tau_{xy}}{\partial y}\right)$$

$$u\frac{\partial v}{\partial x}+v\frac{\partial v}{\partial y}+\frac{\partial p}{\partial y}-\theta=Pr^{\frac{1}{2}}Ra^{\frac{-1}{2}}\left(\frac{\partial \tau_{yy}}{\partial y}+\frac{\partial \tau_{yx}}{\partial x}\right) \quad (12)$$

$$u\frac{\partial \theta}{\partial x}+v\frac{\partial \theta}{\partial y}-(Ra.Pr)^{-1/2}\left(\frac{\partial^2\theta}{\partial x^2}+\frac{\partial^2\theta}{\partial y^2}\right)=0$$

Where λ is a large constant. To solve these equations, initial values of velocity are imposed, then the shear rate and shear stress are evaluated. From the stress tensor, new values of velocity and then, from the energy equation, new values of the temperature can be computed. These steps are repeated until the convergence of velocity and temperature fields. Further details of the method can be found in [18].

3.2. Numerical method validation

A mesh analysis procedure was examined to guarantee a grid independent solution of the present study. Two cases ($Ra = 10^6, Pr = 10$) and ($Ra = 10^6, Pr = 1000$) for both Casson and Bingham fluids are tested, and the comparison is done on the values of the average Nusselt number $\overline{Nu}$. One finds that the mesh consisting in 5985 nodes guarantees a grid independent solution within the relative tolerance level of 10^{-5}.

In order to ensure convergence of results in the case of viscoplastic fluid, the convergence of the solutions has been checked by varying the penalty and regularization parameters. Results show that $\overline{Nu}$ converges within 0.1% by varying λ from 10^3 to 10^4 and also by varying m from 10^3 to 10^4. In the following, all results are obtained for $\lambda = 10^4$ and $m = 10^4$.

Finally, the numerical code has been validated by comparing our results obtained with the Bingham model with results obtained by Turan et al. [9]. Results are depicted in Fig 3 for $Ra = 10^5, 10^6$ and $Pr = 10$. One can notice an excellent agreement in results.

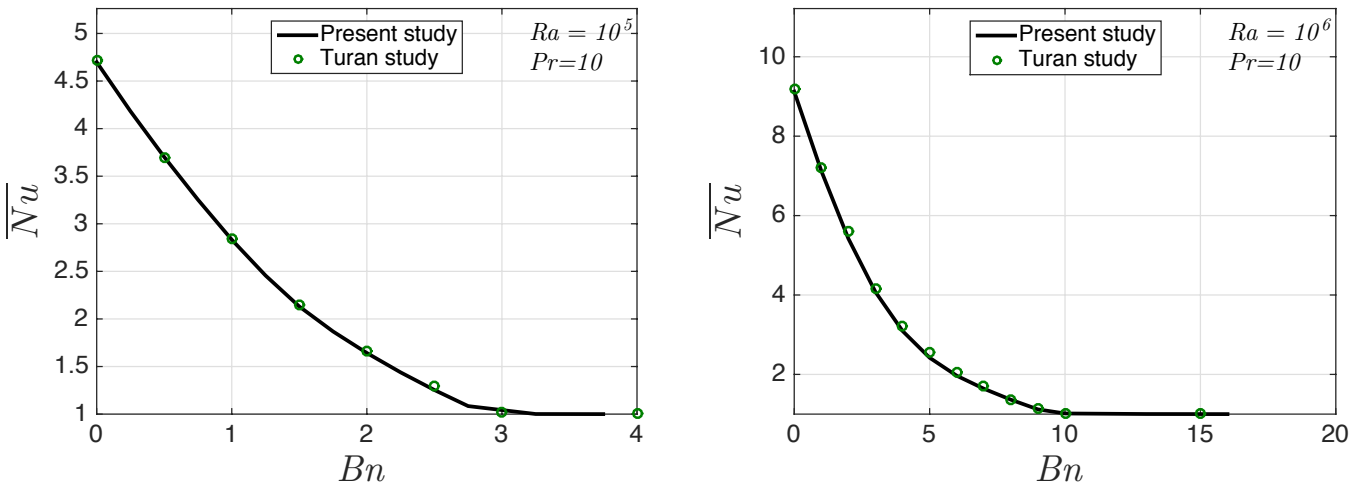

Fig. 3 Mean Nusselt number Nu for Bingham fluids at $Ra = 10^5$ *(left) and* $Ra = 10^6$ *(right) and* $Pr = 10$ *(line: present study, points: Turan study [9]).*

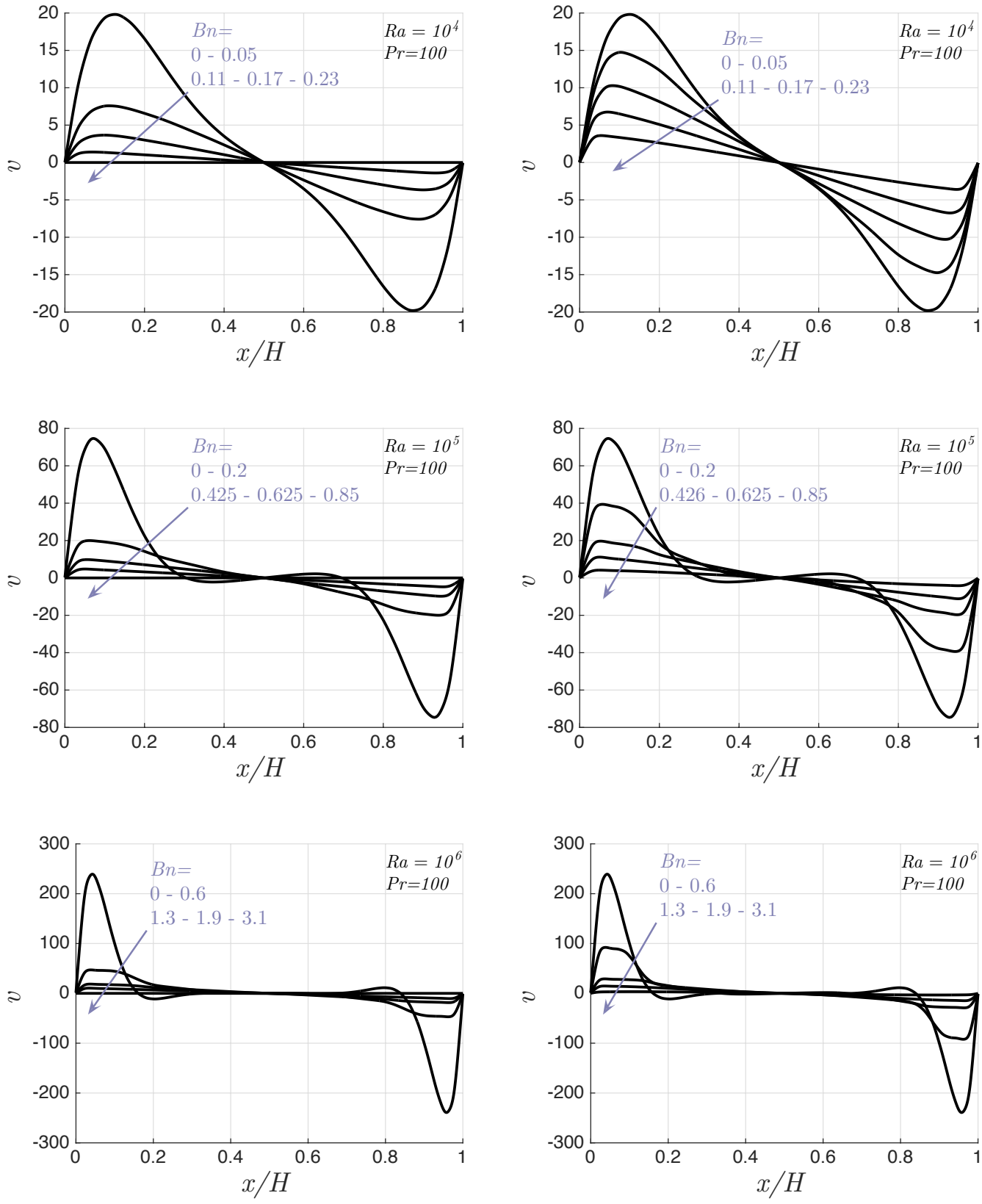

Fig. 4 Variations of non-dimensional velocity v with Bingham number Bn along the horizontal mid-planes for different values of Ra at $Pr = 100$. (Left: Casson model, Right: Bingham model)

4. Results and discussion

4.1. Velocity and temperature

Flow features are given by the coupling velocity and temperature fields. In order to display these features, we present, in Figs. 4 and 5 respectively, the variations of non-dimensional vertical component of velocity v as well as the temperature profiles along the horizontal mid-plane of the cavity for different values of Ra and Bn. We have verified that results are not sensitive to the Prandtl values in the range $Pr = 10 - 10^3$. For this, the Ra and Y numbers are fixed; we observe that results, obtained for each model, are similar when Pr varies. All results depicted in the following are obtained for $Pr = 100$. Results are presented for both Casson (left) and Bingham (right) fluids at similar conditions. The Newtonian case corresponds to $Bn = 0$. For non-zero values of Bn, the Bingham model leads to larger values of velocity compared with the Casson model. Indeed, the ratio between the maximal velocity values of v obtained with the Bingham model and the Casson one is close to 2. It denotes a larger intensity of convection in the Bingham case. A similar tendency is obtained considering the horizontal temperature profiles as depicted in Fig. 5 in which a bit larger variation of θ is observed in the Bingham case. This phenomenon is also clearly highlighted in Figs 6-8 where iso-contours of the non-dimensional temperature θ is depicted for the Newtonian case ($Bn = 0$) and more specifically for both the Casson and Bingham models at different Ra values. Finally, the Bingham model is more destabilizing than the Casson one. This comes from a larger degree of shear-thinning in the Bingham case as underlined in section 2.

On the other hand, for both models, a stabilizing effect of the yield stress is observed. When Bn increases, at fixed Ra and Pr values, variations of velocity and temperature decrease significantly, leading to a decreasing convective intensity. Furthermore, as expected, the increase in Ra values induces an increase in the magnitude of velocity as well as an increase in the temperature variations at fixed Bn values.

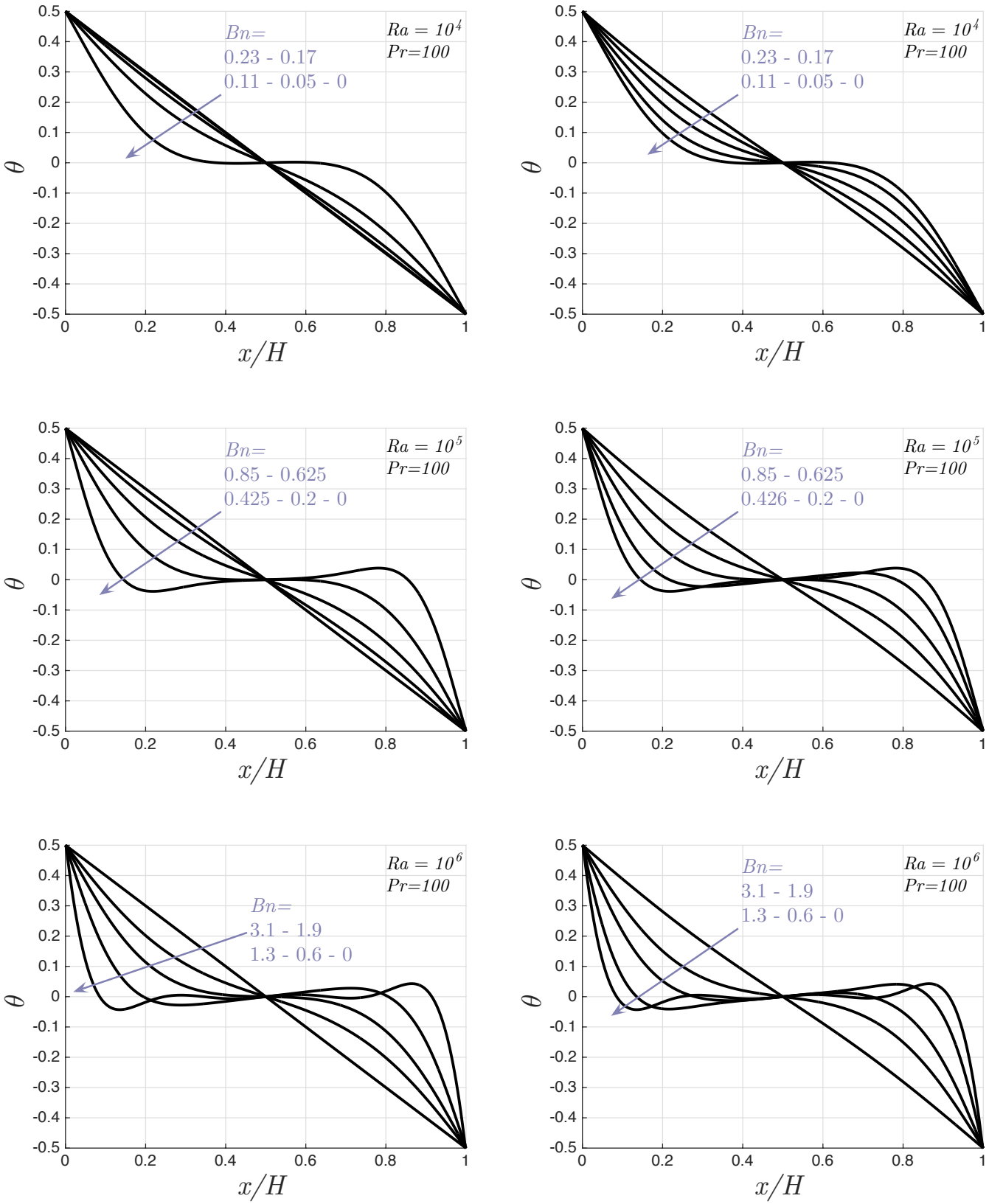

Fig. 5 Variations of non-dimensional Temperature θ with Bingham number Bn along the horizontal mid-planes for different values of Ra at $Pr = 100$. (Left: Casson model, Right: Bingham model)

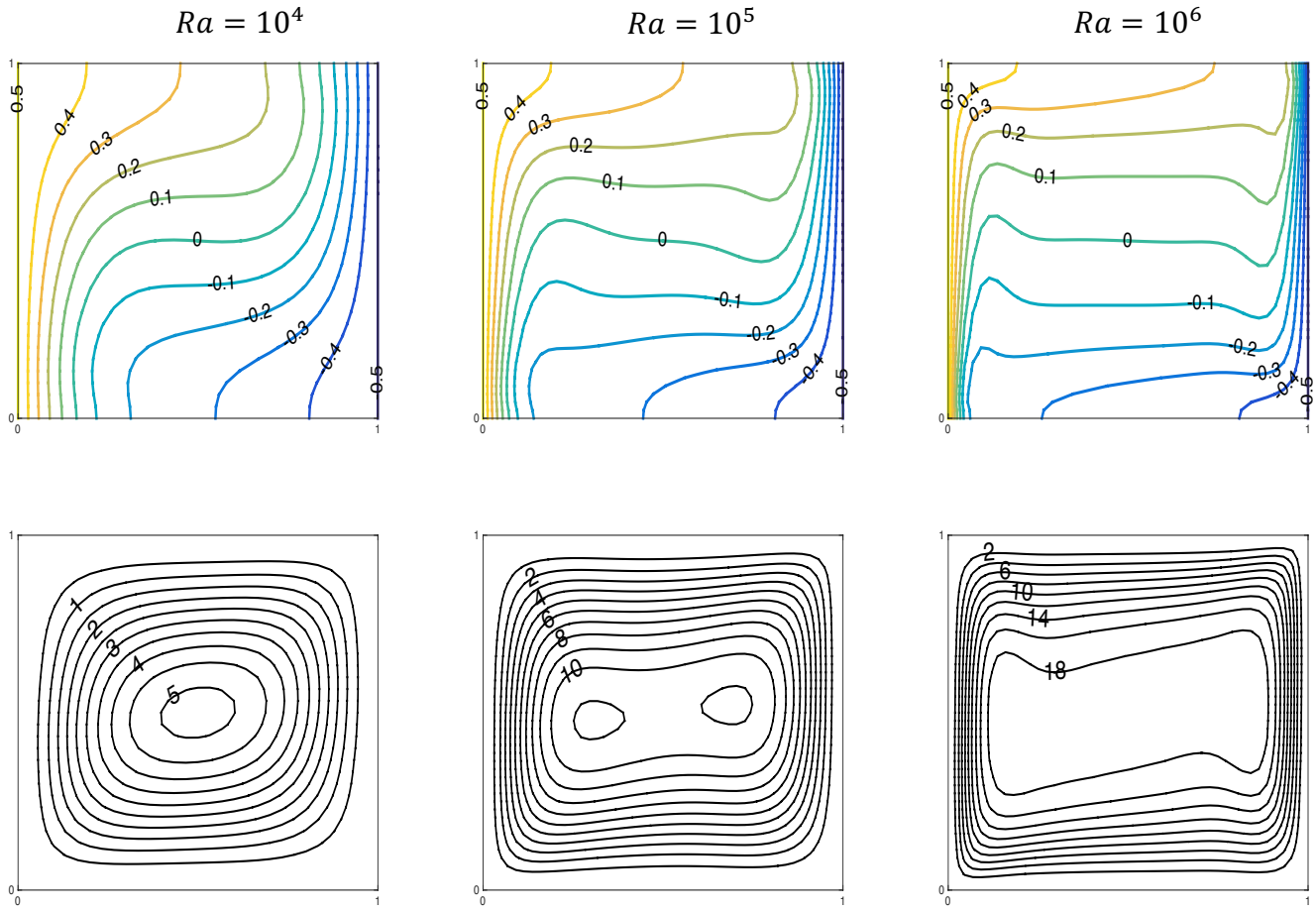

Fig. 6 Contours of non-dimensional temperature θ (top) and stream functions ψ (below) for Newtonian fluids ($Bn = 0$) at $Ra = 10^4$ (left), $Ra = 10^5$ (center) and $Ra = 10^6$ (right).

4.2.Flow structure

The contours of non-dimensional stream functions of Casson and Bingham fluids are displayed in Figs. 9 and 10 respectively. As previously, it is observed that increasing the yield stress (Bn or Y) decreases the magnitude of stream function which confirms the stabilizing effect of the yield stress. Larger values of stream functions can be observed in the Bingham. case

Interestingly, the stabilizing effect of the yield stress via Bn is accompanied by the increase in the plug regions where $\tau < \tau_y$ as represented by the shaded regions in Figs. 9 and 10. For both

the Bingham and Casson models, the unyielded regions has been obtained using a similar regularization and a similar value of the regularized parameter m. In this sense, a comparison of the resulting topology can be done. Two types of plug regions can be distinguished: The Truly Unyielded Regions (TUR) and the Apparently Unyielded Regions (AUR). These latter's regions located in the corners of the cavity and correspond to dead zones without any deformation [12]. Considering the TUR, it is worth noting that they are moving since the velocity is not zero except when the Bn value is such large that no yielded region exists in the cavity and the motion has stopped leading to a motionless conductive regime. This motionless state is particular to the yield stress fluids since for Newtonian fluids, provided that $Ra \neq 0$, there always exists convection in a cavity heated from one side wall. Results obtained in the Bingham fluid case are qualitatively similar than that provided by Turan et al [9] and Huilgol and Kefayati [11]. Comparing the unyielded region between the two models shows that AUR in Bingham model occupy more space than in the Casson model. Comparing both models, the Truly Unyielded Regions are close in terms of shape and area. Some differences can be observed: in the Casson model, the unyielded regions are less numerous than in the Bingham model case, especially in the first diagonal of the cavity (defined by $y = x$). This is due to a larger shear rate $\dot{\gamma}$ in the Bingham case, as shown in Fig. 11. This figure represents the distribution of the second invariant of the shear rate tensor for both Bingham (upside) and Casson (downside) cases at $Ra = 10^5$.

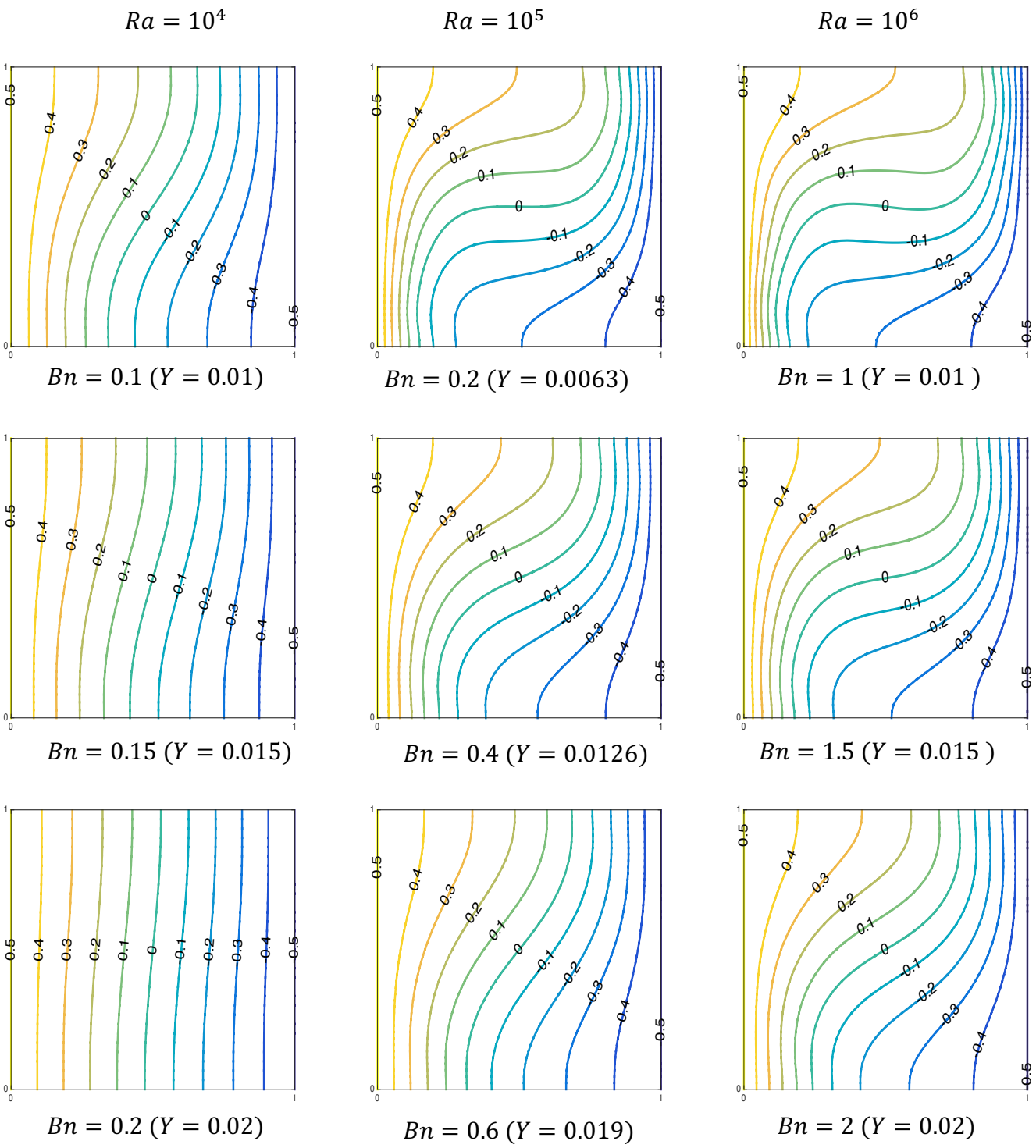

Fig. 7 Contours of non-dimensional temperature θ for different values of Bn at $Ra = 10^4$ (left), $Ra = 10^5$ (center) and $Ra = 10^6$ (right). (Casson model)

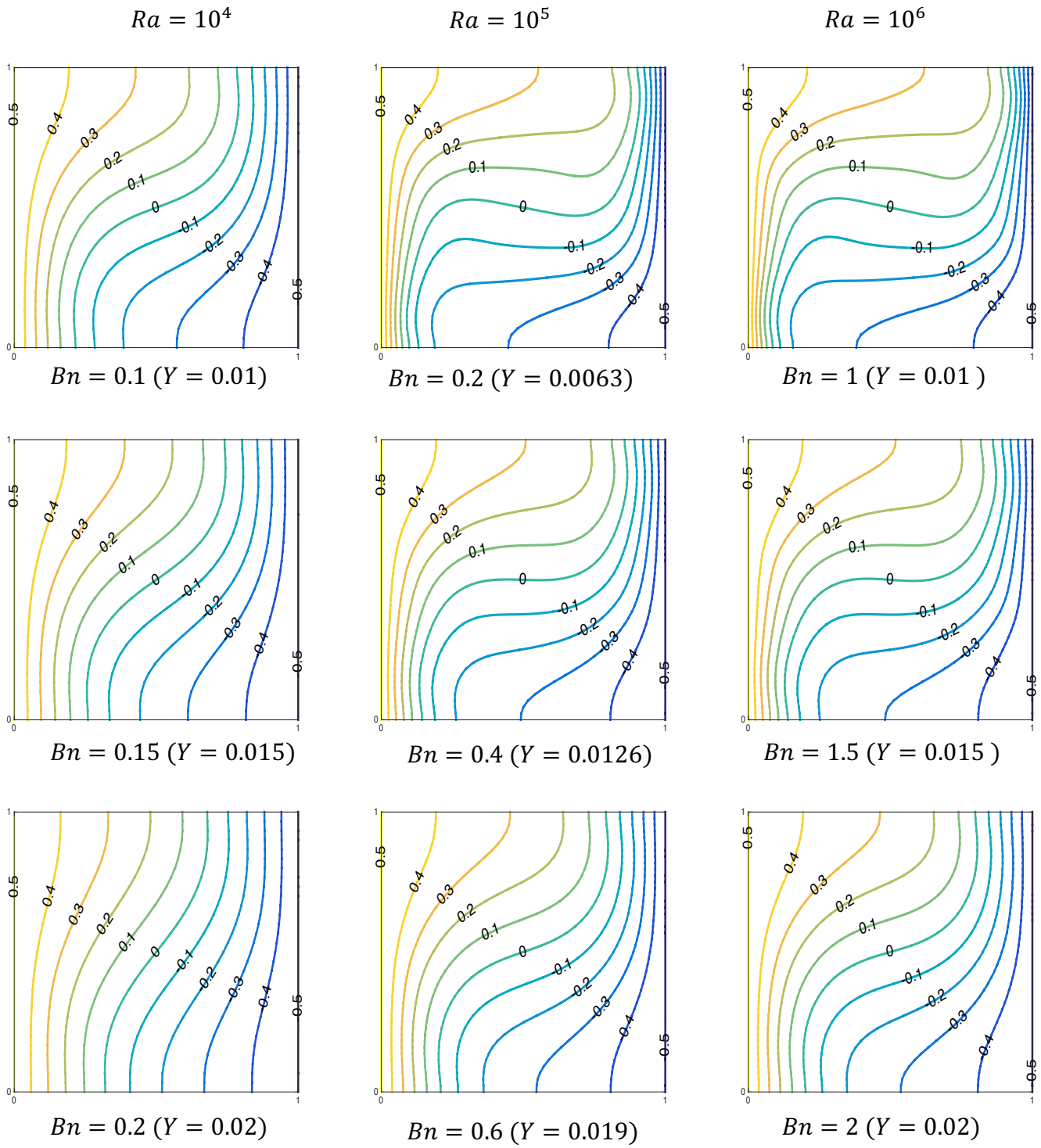

Fig. 8 Contours of non-dimensional temperature θ for different values of Bn at $Ra = 10^4$ (left), $Ra = 10^5$ (center) and $Ra = 10^6$ (right). (Bingham model)

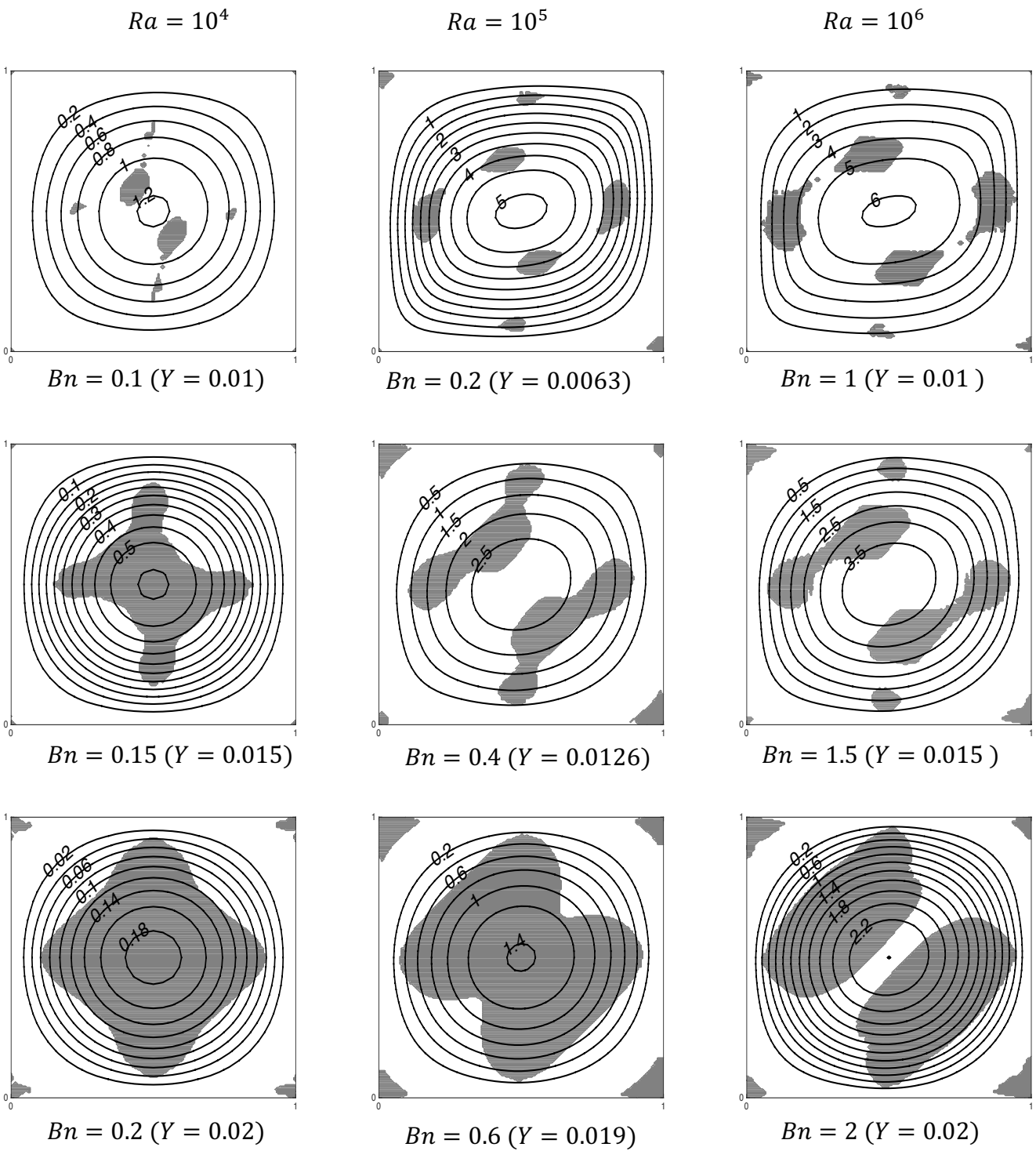

Fig. 9 Contours of non-dimensional stream functions ψ and unyielded zones (gray) for different values of Bn at $Ra = 10^4$ (left), $Ra = 10^5$ (center) and $Ra = 10^6$ (right). (Casson model)

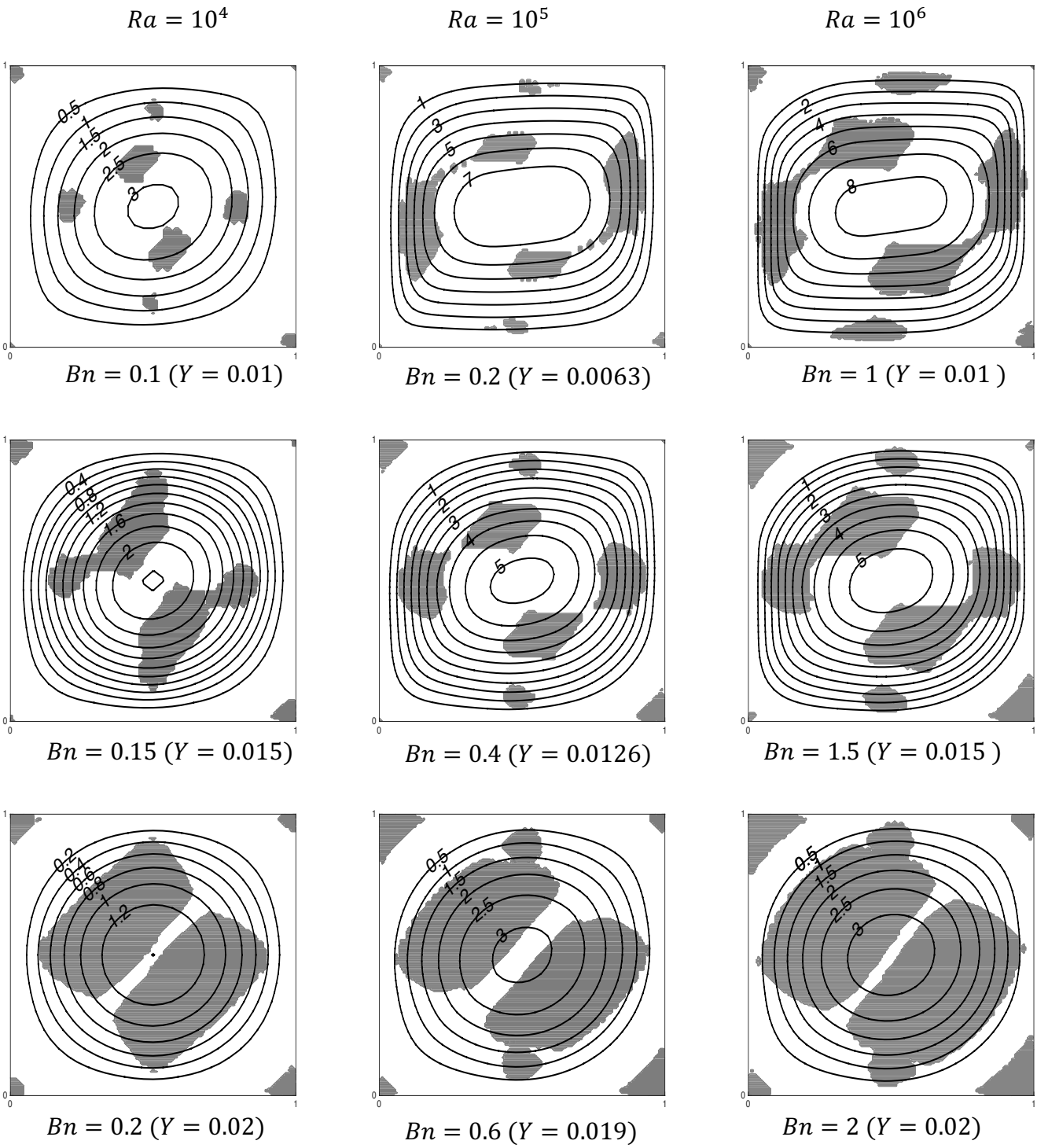

Fig. 10 Contours of non-dimensional stream functions ψ and unyielded zones (gray) for different values of Bn at $Ra = 10^4$ (left), $Ra = 10^5$ (center) and $Ra = 10^6$ (right). (Bingham model).

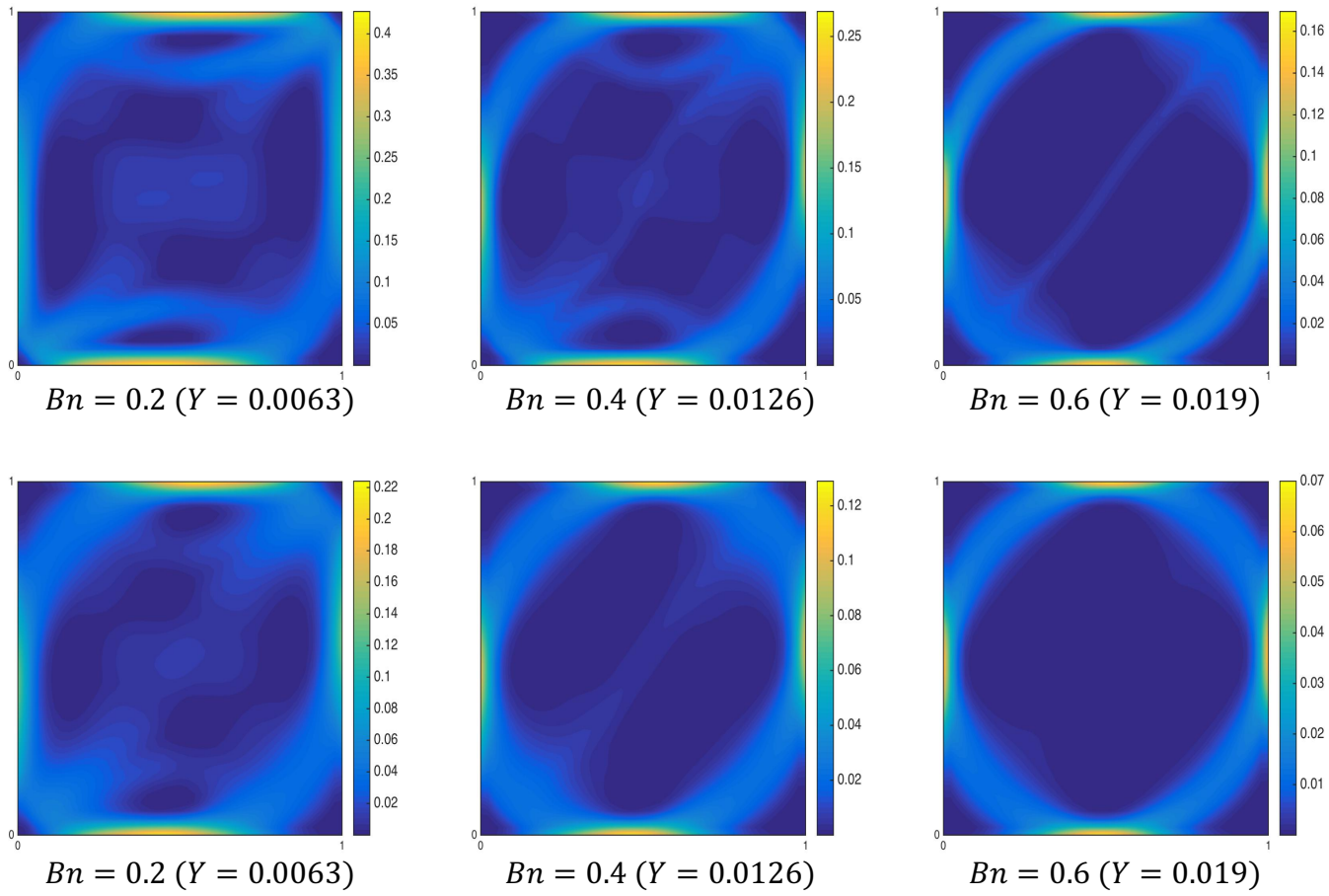

Fig. 11 Distribution of the shear rate $\dot{\gamma}$ for Bingham (top) and Casson (below) models at $Ra = 10^5$.

In Fig. 11, the dark blue regions correspond to values of $\dot{\gamma}$ which converge to zero, leading to unyielded regions. As expected, maximal values of shear rate are obtained at walls. Furthermore, results show that Bingham fluids lead to larger $\dot{\gamma}$ values in the cavity than Casson fluids. This is in agreement with the previous considerations.

4.3.Heat transfer (Nusselt number)

The variation of the mean Nusselt number $\overline{Nu}$ with the Bingham number Bn and the Yield number Y is shown in Fig. 12 for different values of Rayleigh number $Ra = 10^3, 10^4, 10^5, 10^6$. We observe that the heat transfer is maximal for Newtonian fluids ($Bn = 0$). For both the Casson and

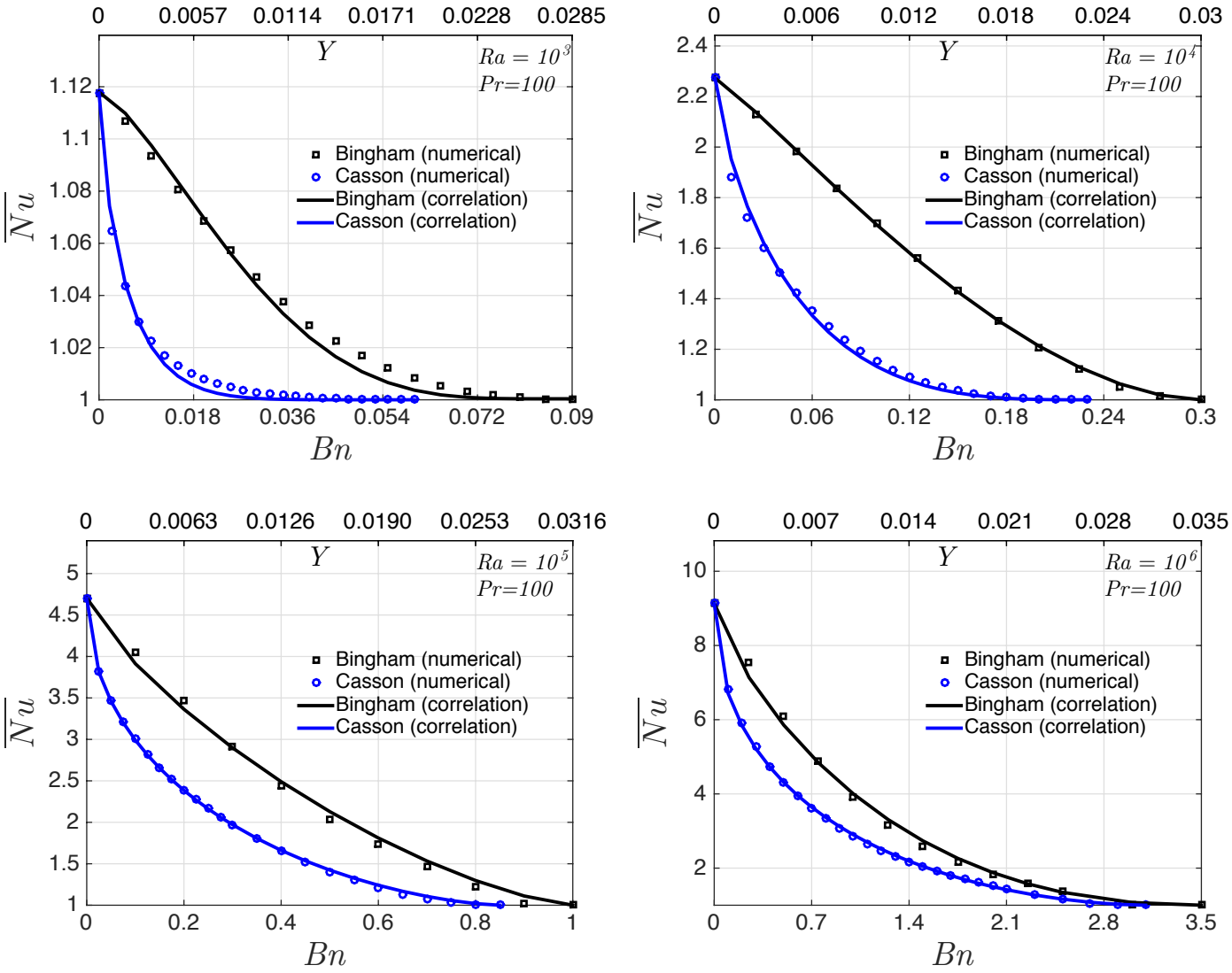

Fig. 12 Evolution of the mean Nusselt number with the Bingham Bn (yield number Y) for four different values of Ra at Pr = 100. [numerical results and prediction of the correlation given by Eq. (13)].

Bingham models, the increase in the yield stress leads to reduce the heat transfer since $\overline{Nu}$ decreases with increasing Bn (or Y) values. Comparing the two viscoplastic fluids, Bingham fluids lead to larger heat transfer than Casson fluids.

On the other hand, whatever the model, for sufficiently large Bn (or Y) values, convection finally stops at Bn_c (or Y_c) and the heat transfer corresponds only to a conductive regime. This is due to the fact that the plug region invades the whole cavity leading finally to a motionless state. In this case, it means that the stresses induced by the horizontal temperature difference are

smaller than the yield stress leading to a solid like behavior in the whole cavity.

Contrary to the Rayleigh-Bénard convection heated from below which leads to a subcritical bifurcation [19], [20], when the cavity is heated from a side wall for either the Casson or the Bingham model, results highlight a supercritical bifurcation since the decrease of the Nusselt number is continuous till the motionless state is reached, i.e. $\overline{Nu} = 1$. Furthermore, the convection stops in Casson fluids for smaller values of Y than in the case of Bingham fluids. This observation is all the more true that the Rayleigh number is such as $Ra \leq 10^5$ as displayed in Fig. 13. For both fluids, results highlight a weak dependence of Y_c with the Rayleigh number: $Y_c \sim Ra^{0.03}$ for Bingham fluids and $Y_c \sim Ra^{0.07}$ for Casson fluids.

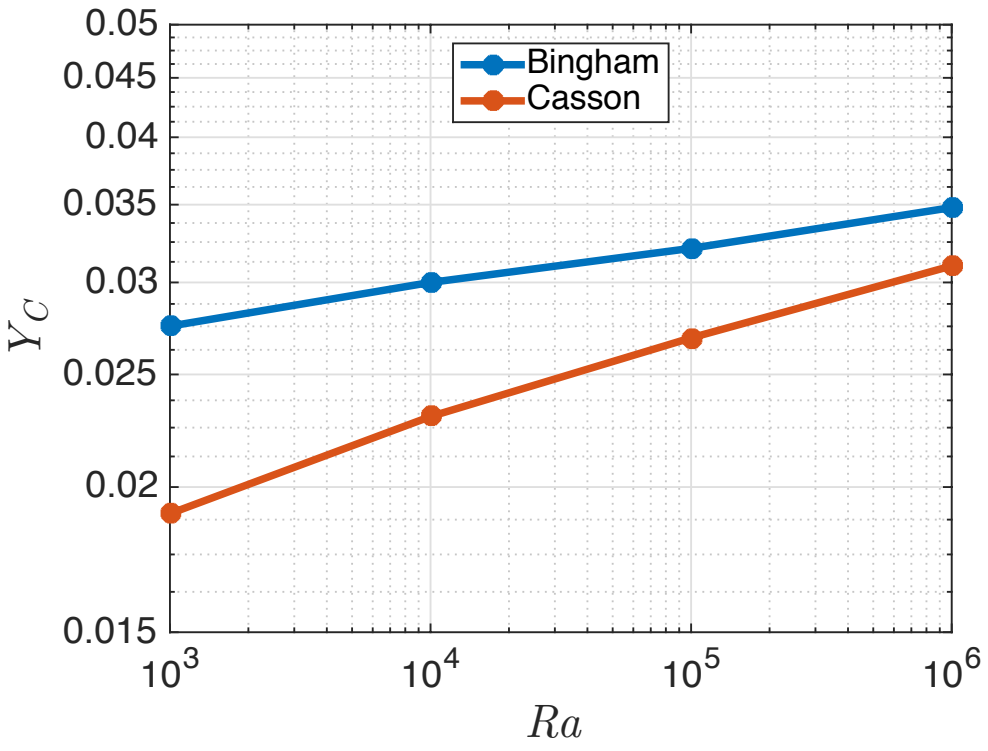

Fig. 13 The variations of critical yield number Y_c with Rayleigh number Ra.

4.3.1 Correlation for the mean Nusselt number

A correlation for the mean Nusselt number $\overline{Nu}$ can be proposed in a general form as below:

$$\overline{Nu} = 1 + (\overline{Nu}_0 - 1)\left[1 - \left(\frac{Y}{Y_c}\right)^a\right]^b \quad (13)$$

where $\overline{Nu}_0$ is the mean Nusselt number obtained in the Newtonian case ($Y = 0$) and Y_c is the critical yield number above which $\overline{Nu} = 1$ (no convection occurs). The values of $\overline{Nu}_0$ and Y_c can be estimated by fitting our numerical results as follows:

$$\overline{Nu}_0 = 0.1495 * Ra^{0.2979} \quad (14)$$

$$Y_c = 0.0231 * Ra^{0.02984} \quad (15)$$

and

$$a = 0.6423 * exp(-6.663 * 10^{-5} * Ra) + 0.7991 * exp(1.14 * 10^{-9} * Ra) \quad (16)$$

$$b = 2.936 * exp(-0.0001853 * Ra) + 1.321 * exp(5.013 * 10^{-7} * Ra) \quad (17)$$

for the Bingham model.

And

$$\overline{Nu}_0 = 0.1495 * Ra^{0.2979} \quad (18)$$

$$Y_c = 0.01185 * Ra^{0.06936} \quad (19)$$

and

$$a = 0.4102 * exp(-1.191 * 10^{-5} * Ra) + 0.3738 * exp(2.575 * 10^{-7} * Ra) \quad (20)$$

$$b = 5.205 * exp(-0.0001233 * Ra) + 1.481 * exp(1.292 * 10^{-7} * Ra) \quad (21)$$

for the Casson model.

The correlation proposed for $\overline{Nu}_0$ in Eq. (14) leads to a mean relative difference with our numerical results which is less than 2% for $10^3 < Ra < 10^6$ as depicted in Fig. 12. These correlations are also very useful in the case of viscoplastic fluids since they provide the heat transfer via Eq. (13) and also Y_c (Eqs. (15) and (19)), the value above which the flow cannot occur. This last value is determined as a function of Ra, with a mean relative difference less than 2%.

5. Conclusions

In this study, a finite element numerical code has been developed to study the laminar natural convection in viscoplastic fluids in a square enclosure with differentially heated side walls. A Casson fluid is studied and compared with a Bingham fluid. For this purpose, a Papanastasiou regularization and a similar value of the regularization parameter ($m = 10^4$) are used for both models. Under these conditions, the degree of shear-thinning is larger when considering a Bingham fluid.

Concerning the natural convection, the effect of the yield stress, via Bn or Y, on heat transfer and flow features are investigated for $10^3 < Ra < 10^6$. Results are not sensitive to the Prandtl number. Because the Casson and Bingham models lead to close values of rheological features (e.g. the viscosity), results are qualitatively the same. It means that the yield stress has a stabilizing effect since the convection can stop while this is not the case for Newtonian fluids. The increase in the yield stress value induces the growth of unyielded regions. Above Y_c (or Bn_c), these regions invade the whole cavity leading to a motionless state. Results highlight a supercritical bifurcation at the transition between the convective and conductive regimes for both models. Differences between the two yield stress models lie in larger values of temperature, velocity magnitude and shear rate in the case of Bingham fluids. The same applies to the convective intensity since larger values of $\overline{Nu}$ are obtained for Bingham fluids. The more destabilizing effect of the Bingham model compared with the Casson model is due to a larger degree of shear-thinning in the Bingham case.

References

[1] S. Ostrach, "Natural Convection in Enclosures," *J. Heat Transfer*, vol. 110, no. 4b, p. 1175, Nov. 1988.

[2] A. Bejan, *Convection Heat Transfer*. Hoboken, NJ, USA: John Wiley & Sons, Inc., 2013.

[3] M. Lamsaadi, M. Naïmi, M. Hasnaoui, and M. Mamou, "Natural Convection in a Vertical Rectangular Cavity Filled with a Non-Newtonian Power Law Fluid and Subjected to a Horizontal Temperature Gradient," *Numer. Heat Transf. Part A Appl.*, vol. 49, no. 10, pp. 969–990, 2006.

[4] O. Turan, A. Sachdeva, N. Chakraborty, and R. J. Poole, "Laminar natural convection of power-law fluids in a square enclosure with differentially heated side walls subjected to constant temperatures," *J. Nonnewton. Fluid Mech.*, vol. 166, no. 17–18, pp. 1049–1063, Sep. 2011.

[5] T. P. Lyubimova, "Numerical investigation of convection in a viscoplastic liquid in a closed region," *Fluid Dyn.*, vol. 12, no. 1, pp. 1–5, Jan. 1977.

[6] A. Vikhansky, "On the onset of natural convection of Bingham liquid in rectangular enclosures," *J. Nonnewton. Fluid Mech.*, vol. 165, no. 23–24, pp. 1713–1716, Dec. 2010.

[7] I. Karimfazli, I. A. Frigaard, and A. Wachs, "A novel heat transfer switch using the yield stress," *J. Fluid Mech.*, vol. 783, pp. 526–566, 2015.

[8] O. Turan, N. Chakraborty, and R. J. Poole, "Laminar Rayleigh-Bénard convection of yield stress fluids in a square enclosure," *J. Nonnewton. Fluid Mech.*, vol. 171–172, pp. 83–96, Mar. 2012.

[9] O. Turan, N. Chakraborty, and R. J. Poole, "Laminar natural convection of Bingham fluids in a square enclosure with differentially heated side walls," *J. Nonnewton. Fluid Mech.*, vol. 165, no. 15–16, pp. 901–913, Aug. 2010.

[10] D. Vola, L. Boscardin, and J. C. Latché, "Laminar unsteady flows of Bingham fluids: A numerical strategy and some benchmark results," *J. Comput. Phys.*, vol. 187, no. 2, pp. 441–456, 2003.

[11] R. R. Huilgol and G. H. R. Kefayati, "Natural convection problem in a Bingham fluid using the operator-splitting method," *J. Nonnewton. Fluid Mech.*, vol. 220, pp. 22–32, 2015.

[12] E. Mitsoulis, “Flows of viscoplastic materials: Models and computations,” *Rheol. Rev.*, vol. 2007, pp. 135–178, 2007.

[13] N. Casson, *Rheology of disperse systems*. Oxford: Pergamon Press, 1959.

[14] R. P. Chhabra and J. F. Richardson, *Non-Newtonian Flow and Applied Rheology*. Elsevier, 2008.

[15] T. C. Papanastasiou, “Flows of Materials with Yield,” *J. Rheol. (N. Y. N. Y).*, vol. 31, no. 5, p. 385, Jul. 1987.

[16] G. Dhatt, G. Touzot, and E. Lefrancois, *Finite Element Method*. Wiley, 2012.

[17] M. S. Aghighi, A. Ammar, C. Metivier, M. Normandin, and F. Chinesta, “Non-incremental transient solution of the Rayleigh–Bénard convection model by using the PGD,” *J. Nonnewton. Fluid Mech.*, vol. 200, pp. 65–78, Oct. 2013.

[18] M. S. Aghighi, A. Ammar, C. Metivier, and M. Gharagozlu, “Rayleigh-Bénard convection of Casson fluids,” *Int. J. Therm. Sci.*, vol. 127C, pp. 79–90, 2018.

[19] C. Li, A. Magnin, and C. Métivier, “Natural convection in shear-thinning yield stress fluids in a square enclosure,” *AIChE J.*, vol. 62, no. 4, pp. 1347–1355, Apr. 2016.

[20] A. Vikhansky, “On the stopping of thermal convection in viscoplastic liquid,” *Rheol. Acta*, vol. 50, no. 4, pp. 423–428, Apr. 2011.